Appl. Phys. A 87, 223–225 (2007)
DOI: 10.1007/s00339-006-3823-6

Applied Physics A
Materials Science & Processing

Z. TANG[1,2,✉]
H. ZHANG[3]
R. PENG[1,2]
Y. YE[2]
C. ZHAO[2]
S. WEN[1]
D. FAN[2]

Subwavelength imaging with two symmetrical interfaces by dielectric-tube photonic crystals

[1] School of Computer and Communication, Hunan University, Changsha 410082, P.R. China
[2] Shanghai Institute of Optics and Fine mechanics, Chinese Academy of Sciences, Shanghai 201800, P.R. China
[3] Department of Optical Science and Engineering, Fudan University, Shanghai 200433, P.R. China

Received: 16 August 2006/Accepted: 16 November 2006
Published online: 22 February 2007 • © Springer-Verlag 2007

ABSTRACT As distinct from coated photonic crystals, in this paper we propose a novel one that is made of dielectric tubes arranged in a close-packet square lattice. Without metallic cores, this structure is low-loss and convenient to fabricate. A left-handed frequency region is found in the second band by dispersion characteristic analysis. Without inactive modes for the transverse electric mode, negative refraction and subwavelength imaging are demonstrated by the finite-difference time-domain simulations with two symmetrical interfaces, i.e. ΓX and ΓM.

PACS 78.20.Ci; 41.20.JB; 42.70.Qs; 41.85.Ct; 42.30.Va

1 Introduction

Photonic crystals (PhCs) are artificial structures whose refractive indexes are periodically arranged [1, 2]. With appropriate design, the propagation of optical waves can be modulated in a controllable manner. For example, superprism and self-collimation have been shown in PhCs experimentally [3, 4]. During the past few years, anomalous electromagnetic phenomena such as negative refraction and flat slab focusing in PhCs have attracted a great deal of attention [5–20]. These phenomena were first predicted in left-handed materials (LHMs), which are characterized by simultaneously negative permittivity and permeability [21]. The most exciting application of LHMs is the realization of the superlens, which can overcome the diffraction limit [22]. Due to the absence of LHMs in nature, various approaches have been proposed to fabricate the equivalent metamaterial [5, 23, 24]. For its controllable dispersion characteristics, PhC can behave as a LHM in some frequency ranges [5].

Negative refraction and flat slab focusing have been demonstrated in many categories of two-dimensional (2D) PhCs [5–17]. Recently, Zhang has studied these anomalous electromagnetic phenomena in 2D coated PhCs, which were fabricated by adding a fraction of a metallic component to the center of each dielectric cylinder [15–17]. Because of the metallic cores, this PhC is poor and inconvenient to fabricate. As an improvement, in this paper we propose a 2D PhC that is made of dielectric tubes arranged in a close-packet square lattice. A left-handed frequency region is found in the second band for the transverse electric (TE) mode. Different from most left-handed PhCs that must be utilized with a specified interface, negative refraction and subwavelength imaging for our structures are demonstrated with two symmetrical interfaces (i.e. ΓX and ΓM) by the finite-difference time-domain (FDTD) simulations [25].

The rest of this paper is organized as follows. In Sect. 2, we theoretically analyze the dispersion characteristics by examining the photonic band structure and equifrequency contours (EFCs). The numerical simulations of the field patterns are shown in Sect. 3. Finally, we summarize this paper in Sect. 4.

2 Dispersion characteristic analysis

Different from coated PhCs, the 2D PhC considered in this paper is made of dielectric tubes arranged in a close-packet square lattice. The dielectric constant of these tubes is $\varepsilon = 12.96$ (e.g., GaAs or Si at 1.55 μm). The inside and outside diameters of each of the tubes are $0.5a$ and a respectively, where a is the lattice constant. Without the metallic components, our PhC is low-loss. In addition, this structure can be fabricated as a PhC fiber.

The photonic band structure and several EFCs for the TE mode are calculated by the plane wave expansion method and plotted in Fig. 1a and b, respectively. The frequency is normalized as a/λ. From these figures, we can see clearly that the PhC behaves as left-handed in the second band [5]. According to group theory the symmetry of these bands is labelled in Fig. 1a. We should mention here that there are A modes on the Σ points in the left-handed frequency region. However, most of previous studied left-handed PhCs were performed for the TM mode with the B modes on the Σ points, which cannot be excited by the incident waves [26]. To excite the Bloch waves effectively, the PhCs must be utilized with a specified interface. Fortunately, such a limitation does not exist for our structures. The effective index $n_{\text{eff}} \approx -1$, which is the optimal frequency for superlensing, is found at the nor-

✉ Fax: +86-21-69918800, E-mail: tangzx1000@163.com

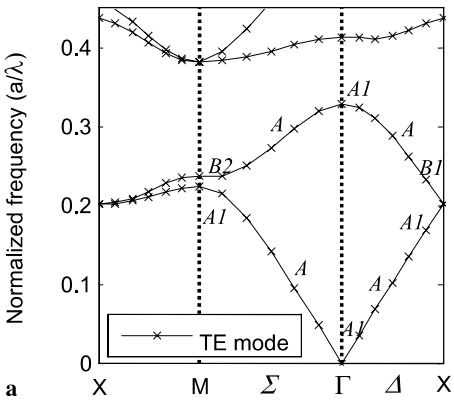

a

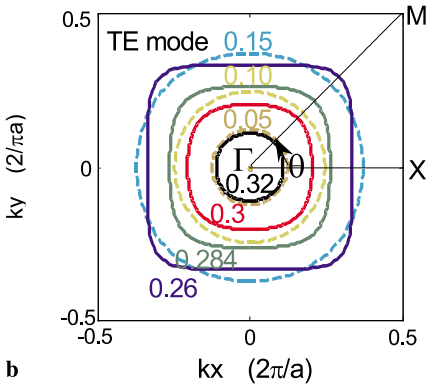

b

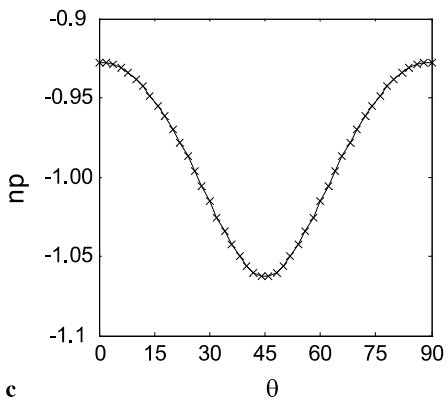

c

FIGURE 1 Dispersion characteristic analysis of the TE mode for the 2D dielectric-tube PhC. (**a**) Photonic band structure; (**b**) several EFCs of the lowest two bands; (**c**) angle-dependent effective index $n_{\text{eff}}(\omega, \theta)$ for the normalized frequency $\omega = 0.284$

malized frequency $\omega = 0.284$. The angle-dependent effective phase index $n_{\text{eff}}(\omega, \theta)$ is plotted in Fig. 1c. Because of near isotropy, $n_{\text{eff}}(\omega, \theta)$ varies between -1.07 to -0.93 with the angle θ.

3 Numerical simulations

To test the above analysis, numerical simulations are performed using the FDTD method with a treatment of perfectly matched layers [27]. Two high symmetrical interfaces between the PhC and free space, i.e. ΓX and ΓM, are employed.

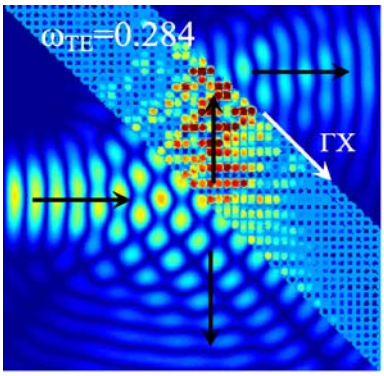

a

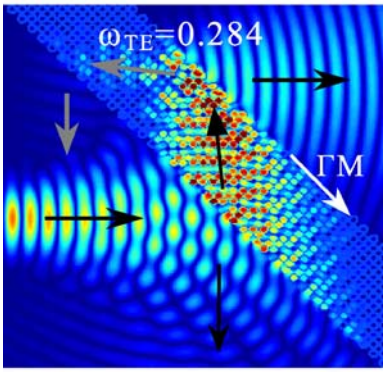

b

FIGURE 2 Negative refractions for the interface along (**a**) ΓX and (**b**) ΓM

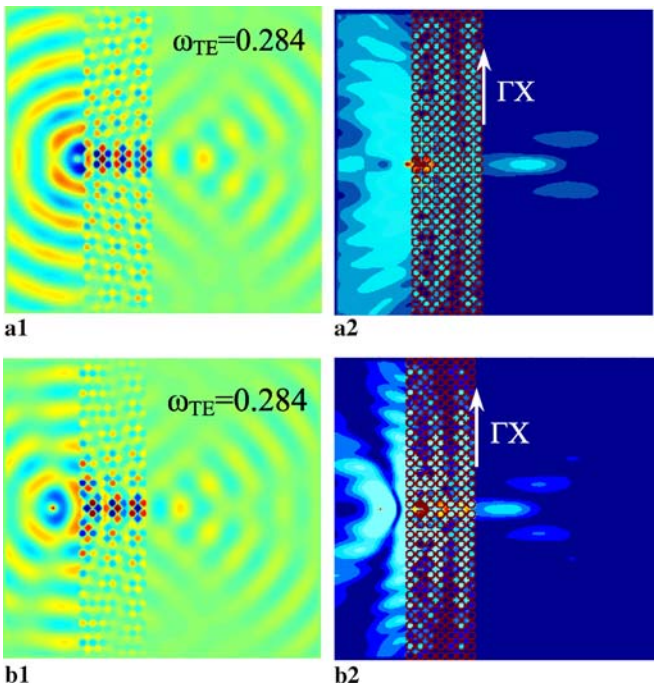

FIGURE 3 Superlensing with the interface along ΓX. (**a**) $d_o = a$, (**b**) $d_o = 3a$. (**a1**) and (**b1**) are snapshots of the magnetic field. (**a2**) and (**b2**) display the average intensities over a period

We first consider a Gaussian beam with a normalized frequency $\omega = 0.284$ incident to the PhC with an angle $\alpha = 45°$ to the interface. Negative refractions for two PhC interfaces along ΓX and ΓM are shown in Fig. 2. It is clear that the incident beams refract negatively almost in the opposite direction

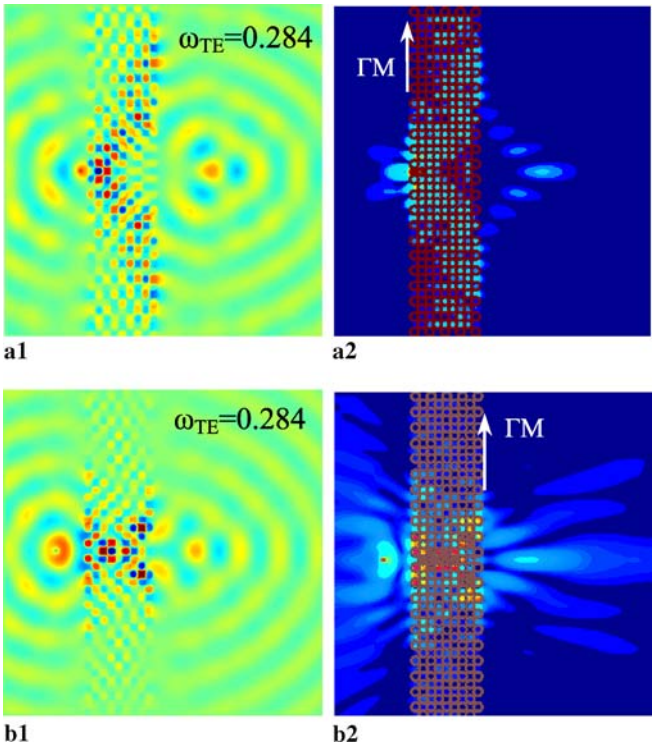

FIGURE 4 The same as Fig. 3, except that the interface of the PhC slab is along ΓM

of their corresponding reflected beams, indicating that the effective index of the PhC is $n_{\text{eff}} \approx -1$. The small discrepancies between Fig. 2a and b can be interpreted with the anisotropy.

Negative refraction allows a flat slab to behave as a lens. More importantly, a flat lens with $n_{\text{eff}} = -1$ can overcome the diffraction limit. Due to A modes on the Σ points, a flat slab made from our structures can act as a superlens with two symmetric interfaces, i.e. ΓX and ΓM, respectively. We take a 7×30 PhC slab as an example. First, we consider that the interface of PhC slab is along the direction of ΓX and locate a continuous-wave point source at $d_{\text{o}} = a$ before the center of the first row. As shown in Fig. 3a, an image is formed at $d_{\text{i}} = 5a$ away from the center of the last row. Then, we move the source to $d_{\text{o}} = 3a$ to see the dependence of the image on the object distance. In Fig. 3b, the image is moved to $d_{\text{i}} = 3.55a$. It is obvious that summation of the object distance and the image distance is almost a constant, which is required by Snell's law for a flat lens with $n_{\text{eff}} \approx -1$. A closer look at the simulation data reveals that the full width at half maximum (FWHM) of the image is 0.426λ.

Finally, we turn the interface to ΓM and perform similar numerical simulations as before. As shown in Fig. 4, the image is formed at $d'_{\text{i}} = 6.14a$ and $d'_{\text{i}} = 4.39a$ for $d_{\text{o}} = a$ and $d_{\text{o}} = 3a$, respectively. The summation of the image distance and the object distance is nearly invariant too. The difference of the propagation maps between Figs. 3 and 4 also resulted from the anisotropy. As more evanescent waves are coupled efficiently for the PhC interface along ΓM, which resulted from the slight flat EFC, the FWHM of the image is improved to 0.398λ [11].

4 Conclusions

In summary, we have systematically investigated a 2D PhC that is made of dielectric tubes arranged in a close-packet square lattice. A left-handed frequency region has been found in the second band by using the plane wave expansion method to analyze the photonic band structure and EFCs. Different from previous left-handed PhCs with inactive modes, negative refraction and subwavelength imaging have been demonstrated by the FDTD simulations with two symmetrical interfaces, i.e. ΓK and ΓM. With the interface along ΓM, better images have been obtained due to the slightly flat EFC. Our analysis has only been focused on a specific structure in this paper, but it can be extended to others such as the dielectric-tube PhC with different dielectric constants and geometric parameters. With appropriate design, another optimal frequency can be found and the superlensing effect can be realized too.

ACKNOWLEDGEMENTS This work is partially supported by the Natural Science Foundation of China (Grant Nos. 10674045), the National High Technology Research and Development Program of China (Grant No. 2004AA84ts12), and the Specialized Research Fund for the Doctoral Program of Higher Education of China (Grant No. 20040532005).

REFERENCES

1 E. Yablonovitch, Phys. Rev. Lett. **58**, 2059 (1987)
2 S. John, Phys. Rev. Lett. **58**, 2486 (1987)
3 H. Kosaka, T. Kawashima, A. Tomita, M. Notomi, T. Tamamura, T. Sato, S. Kawakami, Phys. Rev. B **58**, 10 096 (1998)
4 H. Kosaka, T. Kawashima, A. Tomita, M. Notomi, T. Tamamura, T. Sato, S. Kawakami, Appl. Phys. Lett. **74**, 1212 (1999)
5 M. Notomi, Phys. Rev. B **62**, 10 696 (2000)
6 C. Luo, S.G. Johnson, J.D. Joannopoulos, J.B. Pendry, Phys. Rev. B **65**, 201 104 (2002)
7 E. Cubukcu, K. Aydin, E. Ozbay, S. Foteinopoulou, C.M. Soukoulis, Nature **423**, 604 (2003)
8 P.V. Parimi, W.T. Lu, P. Vodo, S. Sridhar, Nature **426**, 404 (2003)
9 Z. Tang, H. Zhang, R. Peng, Y. Ye, L. Shen, S. Wen, D. Fan, Phys. Rev. B **73**, 235 103 (2006)
10 M. Qiu, S. Xiao, A. Berrier, S. Anand, L. Thylén, M. Mulot, M. Swillo, Z. Ruan, S. He, Appl. Phys. A **80**, 1231 (2005)
11 P.A. Belov, C.R. Simovski, P. Ikonen, Phys. Rev. B **71**, 193 105 (2005)
12 R. Moussa, S. Foteinopoulou, L. Zhang, G. Tuttle, K. Guven, E. Ozbay, C.M. Soukoulis, Phys. Rev. B **71**, 085 106 (2005)
13 Z. Tang, R. Peng, D. Fan, S. Wen, H. Zhang, L. Qian, Opt. Express **13**, 9796 (2005)
14 S. Yang, T. Xu, H. Ruda, M. Cowan, Phys. Rev. B **72**, 075 128 (2005)
15 X. Zhang, Phys. Rev. B **70**, 195 110 (2004)
16 X. Zhang, L.-M. Li, Appl. Phys. Lett. **86**, 121 103 (2005)
17 X. Zhang, Phys. Rev. B **70**, 205 102 (2005)
18 C. Luo, S.G. Johnson, J.D. Joannopoulos, Appl. Phys. Lett. **81**, 2352 (2002)
19 X. Ao, S. He, Opt. Lett. **29**, 2542 (2004)
20 Z. Lu, J.A. Murakowski, C.A. Schuetz, S. Shi, G.J. Schneider, D.W. Prather, Phys. Rev. Lett. **95**, 153 901 (2005)
21 V.G. Veselago, Sov. Phys. Uspekhi **10**, 509 (1968)
22 J.B. Pendry, Phys. Rev. Lett. **85**, 3966 (2000)
23 D.R. Smith, W.J. Padilla, D.C. View, S.C. Nemat-Nasser, S. Schultz, Phys. Rev. Lett. **84**, 4184 (2000)
24 G.V. Eleftheriades, A.K. Iyer, P.C. Kremer, IEEE Trans. Microw. Theory Technol. **50**, 2702 (2002)
25 A. Taflove, *Computational Electrodynamics: The Finite-Difference Time-Domain Method*, 2nd ed. (Artech House, Norwood, 2000)
26 K. Sakoda, *Optical Properties of Photonic Crystals*, Springer Ser. Opt. Sci. (Springer, Berlin, 2001)
27 J.P. Berenger, J. Comput. Phys. **114**, 185 (1991)